AD NUMBER

AD832715

NEW LIMITATION CHANGE

TO

Approved for public release, distribution unlimited

FROM

Distribution authorized to U.S. Gov't. agencies and their contractors; Critical technology; Apr 1968. Other requests shall be referred to Flight Dynamics Labaoratory [FDDA], Wright-Patterson AFB, OH, 45433.

AUTHORITY

AFFDL ltr, 29 Oct 1973

AFFDL-TR-67-167

PREDICTION OF BOUNDARY LAYER PRESSURE FLUCTUATIONS

M. V. LOWSON

WYLE LABORATORIES

TECHNICAL REPORT AFFDL-TR-67-167

APRIL 1968

AIR FORCE FLIGHT DYNAMICS LABORATORY
AIR FORCE SYSTEMS COMMAND
WRIGHT-PATTERSON AIR FORCE BASE, OHIO

1

40

NOTICE

When Government drawings, specifications, or other data are used for any purpose other than in connection with a definitely related Government procurement operation, the United States Government thereby incurs no responsibility nor any obligation whatsoever; and the fact that the Government may have formulated, furnished, or in any way supplied the said drawings, specifications, or other data, is not to be regarded by implication or otherwise as in any manner licensing the holder or any other person or corporation, or conveying any rights or permission to manufacture, use, or sell any patented invention that may in any way be related thereto.

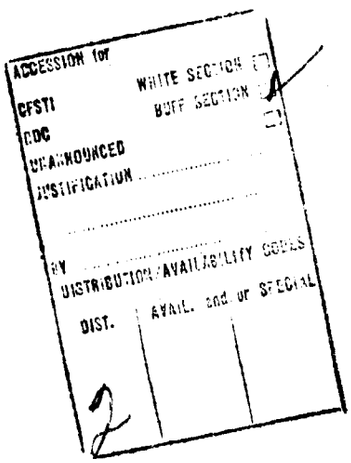

Copies of this report should not be returned unless return is required by security considerations, contractual obligations, or notice on a specific document.

200 - May 1968 - CO455 - 34-721

AFFDL-TR-67-167

PREDICTION OF BOUNDARY LAYER PRESSURE FLUCTUATIONS

M. V. LOWSON

TECHNICAL REPORT AFFDL-TR-67-167

FOREWORD

The research effort reported herein was performed by the Testing Division of Wyle Laboratories, Huntsville, Alabama, under AF Contract F33(615)-67-C-1287. This contract was initiated under Project No. 1471, "Aero-Acoustic Problems" and Task No. 147102, "Prediction and Control of Noise" of the Air Force System Command's exploratory development program. The work was administered under the direction of the Air Force Flight Dynamics Laboratory. Mr. D. L. Smith was the project engineer.

This report covers work performed during the period of December 1966 to January 1968. The manuscript of this report was released by the author in January 1968 for publication as an AFFDL Technical Report. Wyle Laboratories Report No. WR 67-15 has also been assigned to this report.

The work to be performed under Contract F33(615)-67-C-1287 concerns the design of aircraft fuselage soundproofing systems. This report covers a portion of this work. It is concerned with predicting the characteristics of the noise generated in turbulent boundary layers. A separate report, AFFDL-TR-68-2, entitled, "Structural Acoustic Response, Noise Transmission Losses and Interior Noise Levels of an Aircraft Fuselage Excited by Random Pressure Fields" will contain the complete results of the contracted research.

This report has been reviewed and is approved.

Howard A. Magrath

HOWARD A. MAGRATH
Chief, Vehicle Dynamics Division
AF Flight Dynamics Laboratory

ABSTRACT

The pressure fluctuations beneath equilibrium boundary layers at subsonic and supersonic speeds are reviewed. Empirical formulae are presented for the intensity, spectra, and cross spectra of the fluctuations. The formulae are intended for direct use in structural response calculations. A simple theoretical model to predict intensities at supersonic speeds is put forward, and the effects of nonequilibrium boundary layers are discussed in general terms. An appendix gives theoretical justification for negative exponential correlation curves at large spacings.

TABLE OF CONTENTS

ILLUSTRATIONS

SECTION I

INTRODUCTION

The pressure fluctuations occurring beneath a turbulent boundary layer on an aircraft in flight have two important results. Firstly, they are the source of cabin internal noise which can disrupt pilot communication and irritate passengers. Secondly, they can cause fatigue failure of the aircraft structure. There is, therefore, considerable interest in accurate prediction of this phenomenon.

Over a considerable portion of the aircraft only the attached boundary layer sources are significant, and these are the only sources considered in this report. Even under this limitation the effects of fuselage geometry and flight condition can still cause significant variation in the observed characteristics. However, little systematic data exists on these effects so that it is usually necessary to assume that the boundary layer is close to the equilibrium condition.

The information required to compute the fuselage response, and thereby the internal noise field, may be classified under three headings.

i) The Overall Level

ii) The Power-Spectrum

iii) The Cross-Spectral Density as a Function of Position.

Thus, in describing the characteristics of the attached boundary layer each of the above features will be discussed separately.

The basic philosophy underlying the prediction methods put forward here is as follows: First of all, the basic mechanisms underlying the phenomenon are studied. These mechanisms are used to suggest nondimensional parameters for collapsing the available data. Where alternatives exist the simplest and most direct method has been preferred. Thus, for example, attached boundary layer pressure fluctuation data has been collapsed using boundary layer thickness (δ) as a typical dimension, because this parameter is both simpler to predict and more related to the flow mechanisms than the displacement or momentum thickness of the boundary layer.

Considerable data has now been accumulated on the subsonic problem, so that the pressure fluctuations occurring in this case can be predicted quite well. However, data for the supersonic problem is far from complete, and predictions for this supersonic case rely more on extrapolations from the better understood subsonic case. Naturally, less confidence can be felt in the supersonic predictions made in this report.

SECTION II

PRESSURE FLUCTUATIONS IN THE ATTACHED TURBULENT BOUNDARY LAYER

1. OVERALL LEVEL

Experimental and theoretical information on the overall level, particularly at supersonic speeds, is fragmentary and not in particularly good agreement. However, reasonably good correlation has been found using p_{rms}/q as a parameter (Reference 1), where p_{rms} is the root mean square pressure fluctuation, and q is the dynamic head ($0.5\ \rho\ U^2$). The accuracy of this prediction is reduced at supersonic speeds. Theory (Reference 2) suggests that p_{rms}/τ_w would be a suitable nondimensionalized parameter, where τ_w is the wall shear stress, but this theoretical prediction is dependent on the similarity of the boundary layer velocity profiles. Neither the effects on pressure fluctuations of roughness (Reference 3) nor those of pressure gradient (Reference 4) are found to be predicted on a τ_w basis. Thus, use of τ_w increases the complexity of prediction without offering any advantages in increased applicability.

Figure 1 shows a comparison of data under the two schemes. The scatter is apparent. An advantage of using τ_w is that $\tau_w = 3.0$ does give a line which is approximately a mean of the various results at both subsonic and supersonic speeds (Figure 1b). However, there is every reason to expect that p_{rms} would be a function of Mach number, so that a graph of p_{rms}/q versus M would be an acceptable predictor if the data could be shown to collapse.

The basic mechanism underlying the production of the surface pressure fluctuations beneath turbulent boundary layer, at least in subsonic flows, appears to be two-fold. Firstly, there is a component associated with the eddies at the edge of the laminar sublayer, tentatively associated with the laminar sublayer "eruption" process (Reference 5). This component is relatively intense, is typically of high frequency, ($\omega\ \delta/U_o > 10$) and has a convection speed of about 0.5 - 0.6 of the free-stream velocity. The second component is associated with the eddies in the outer intermittent parts of the boundary layer. The intensity of this component appears to be markedly affected by upstream conditions such as roughness or protuberances, is typically of low frequency ($\omega\delta/U_o \sim 1.0$), and has a convection speed of about 0.8 of the of the free-stream velocity. The experimental data which shows these effects in the clearest manner is that of Bull (Reference 6). The relative effectiveness of these two mechanisms at supersonic speeds is not known, but Black, in unpublished work, has been able to collapse subsonic and supersonic data by using arguments based on the above physical picture. Furthermore, the anti-correlation between temperature and velocity fluctuations in a supersonic boundary layer (Reference 7) suggests that the eruption of hot, low velocity eddies from the wall is still an important feature in that case.

At subsonic speeds the wall layer is generally the most effective source of fluctuating pressures. The assumption that this will be true at supersonic speeds leads to an interesting result for the intensity. At subsonic speeds the available data suggests that the fluctuating pressure intensity is given approximately by

$$p_{rms} = 0.006 \times (0.5\ \rho_o\ U^2) \tag{1}$$

where $0.5\ \rho_o\ U^2$ is the dynamic head (q) with ρ_o the free-stream density and U the velocity. Assuming that the wall layer is the principal source of fluctuating pressure at supersonic speeds suggests the following universal formula

$$p_{rms} = 0.006 \times (0.5\ \rho_1\ U^2) \tag{2}$$

where ρ_1 is the density near the wall at the site of the most intense eddies. Maintaining U as the free-stream velocity implies the subsidiary assumption that the turbulent velocities are always proportional to U, and that there is no change of relative scale. This feature agrees with arguments put forward by Morkovin (Reference 7). Since the temperature increases and the density decreases near the wall, Equation (2) suggests a reduction in the value of p_{rms}/q at supersonic speeds. This observation has been the subject of unpublished work by both Eldred and Houbolt.

Now

$$\frac{\rho_1}{\rho_o} = \frac{T_o}{T_1}$$

for constant static pressure through the boundary, thus:

$$p_{rms}/q = 0.006\ T_o/T_1 \tag{3}$$

For an adiabatic (nonconducting) wall

$$\frac{T_{aw}}{T_o} = 1 + R \left\{ \frac{\gamma - 1}{2} \right\} M^2 \tag{4}$$

Where, for a typical turbulent boundary layer, the recovery factor $R \approx 0.9$ (Reference 8, Page 1123).

Then, using the Crocco equation for the temperature velocity relation, which applies to a flow with a Prandtl number of unity, (Reference 8, Equation 26.12),

$$\frac{T_1}{T_o} = \frac{T_w}{T_o} + \left\{1 - \frac{T_w}{T_o}\right\} \frac{U_1}{U_o} + \frac{(\gamma - 1)}{2} M^2 \left(1 - \frac{U_1}{U_o}\right) \frac{U_1}{U_o} \qquad (5)$$

and substituting from (4) assuming an adiabatic wall

$$\frac{T_1}{T_o} = 1 + \left(1 - \frac{U_1}{U_o}\right)\left(R + \frac{U_1}{U_o}\right) \frac{(\gamma - 1)}{2} M^2 \qquad (6)$$

Now suppose that the principal source of the pressure fluctuation occurs at $U_1 = 0.5\, U_o$ (the edge of the laminar sublayer), then

$$\frac{T_1}{T_o} = 1 + 0.14\, M^2 \qquad (7)$$

assuming $R = 0.9$, $\gamma = 1.4$. Thus, Equations 3 and 7 suggest

$$p_{rms}/q = 0.006/(1 + 0.14\, M^2) \qquad (8)$$

as an empirical curve for the fluctuating pressure intensity beneath an attached turbulent boundary layer. This curve is plotted in Figure 1a, and can be seen to be a fairly good, slightly conservative fit to the available data. Thus, Equation 8 is recommended for prediction.

It may be noted that the data of Kistler and Chen (Reference 9) does not appear on Figure 1a. These were the first measurements made for the supersonic case, and have been used by many authors. However, their results are much above later experiments, and furthermore, their spectra have a much larger high frequency content than later investigations (Reference 10). Possibly wind tunnel noise, or a nonequilibrium boundary layer was the cause of this discrepancy. The later data now available, particularly Reference 11, suggests that these initial results of Kistler and Chen be discarded. However it should be pointed out that the results from Speaker and Ailman (Reference 11) have been interpolated (on a constant Re_θ basis) from quite widely varying data points at each Mach number.

Figures 1a and 1b show that there is reasonable agreement between the prediction curve suggested here and that using $p_{rms}/\tau_w = 3.0$, using Bies' methods for predicting τ_w (Reference 10). Bies' method for predicting τ_w again uses the heating of the layer near the wall as the key effect although in this case the temperature affects the result through the viscosity rather than the density. Thus, the agreement between the two curves results basically from the same temperature

effect, although the analytical result of the present method is thought to be somewhat simpler to apply. If the wall is heated or cooled then the wall layer will change in density and a change in pressure fluctuation intensity would be predicted. Calculations of the effect have been made from the formula

$$\frac{T_1}{T_o} = 0.5\,(T_w/T_{aw} + 1) + 0.1\,M^2\,(0.9\,T_w/T_{aw} + 0.5) \qquad (9)$$

This is derived directly from the equations above after putting $\gamma = 1.4$, $R = 0.9$. T_w is the actual wall temperature. In practice the wall will always be cooled, and it is unlikely that T_w/T_{aw} will be less than 0.8. A graph of the predicted effect on p_{rms}/q is shown in Figure 2, and the effect can be seen to amount to about one dB. It therefore seems unlikely that this effect can justify inclusion in a general calculation.

The empirical formula, Equation 8, can be rewritten as

$$p_{rms} = \frac{0.0042\ p_o}{M^{-2} + 0.14} \qquad (10)$$

where p_o is the free stream static pressure. Thus, as M becomes very large $p_{rms} \rightarrow 0.03\ p_o$. Use of a formula such as (1) would suggest intensities several orders of magnitude greater than this. Physically it does seem reasonable that the limiting intensity of the fluctuating pressure sources would be proportional to the static pressure. This general conclusion may also apply to other fluctuating pressure sources at high Mach numbers.

2. SPECTRAL DISTRIBUTION

The frequency spectra of attached turbulent boundary layer pressure fluctuations are found to scale on a Strouhal number basis; that is the frequency is nondimensionalized by multiplying a typical length and dividing by a typical velocity. However, choice of correct typical lengths and velocities is far from easy. Free-stream velocity is generally used for the nondimensionalized velocity, although the use of the typical eddy convection velocity, itself a function of frequency, would correspond more closely with the physical situation. For simplicity, free stream velocity will be used here.

Definition of a typical length is more difficult. Boundary layer thickness (δ), displacement thickness (δ^*), and momentum thickness (θ) have all been used by various authors. For subsonic boundary layers most results have been taken for equilibrium flows with a similar ratio of these characteristic lengths, so that nondimensionalization using any of these gives very similar collapse. In supersonic flows the typical lengths do vary widely with Mach number, but no final conclusion can be drawn on

the relative merits of the collapse against any particular length. Perhaps the most generally used typical length is δ^*, the displacement thickness. However, in this report the boundary layer thickness δ will be used for three reasons: firstly, it is easier to predict; secondly, it is related to a physical characteristic of the flow, the size of the largest eddies; and thirdly, it gives a slightly improved collapse of the only available supersonic data. It should be noted that Black (Reference 12) has achieved a reasonably good collapse of a widely varying spectra by using $(\omega\nu/U_\tau^2)$ as a nondimensional frequency, where ω is the circular frequency, ν the kinematic viscosity, and U_τ shear velocity. The use of this parameter was suggested by the idea that laminar sublayer eruption was a leading source of the pressure fluctuations (see also Reference 5). The success of the above parameter is somewhat surprising at first sight, but writing

$$\frac{\omega\nu}{U_\tau^2} = \left(\frac{\omega\nu\rho}{\tau_w}\right) = \omega\left(\frac{\partial u}{\partial y}\bigg|_{y=0}\right)^{-1}$$

shows that it is equivalent to the nondimensionalizing the frequency by the slope of the velocity profile at the wall. This seems not unreasonable physically, even if the original sublayer eruption hypothesis is not true. This nondimensionalization scheme has not been used in this report since it is complex to apply and does not give good collapse over either the high or low frequency parts of the spectrum, although it is successful over the region of maximum power production.

The principal problem in predicting subsonic spectra under any scheme is estimation at the low frequencies. Experiment, both in flight and in wind tunnels, shows considerable low frequency scatter from the very low values reported by Hodgson (Reference 13) for a glider to the high values reported by Gibson (Reference 14) and Maestrello (Reference 15) for full scale aircraft, although Hodgson's results were taken at low Reynolds numbers on a far from equilibrium boundary layer and should probably be discounted. It is extremely difficult to define any single curve from the available data. Bies has recently published a detailed review of spectral measurements in a wind tunnel and in flight (Reference 10) and suggested the curves shown in Figure 3 as means through the data. The scatter about these curves is about $\pm$ 5 dB. The curves in Figure 3 have been converted to the present basis by assuming that the wind tunnel results were taken at typical Mach number of 0.5 and a typical Reynolds number of 10^7, while the flight results were typified by the values $M = 0.8$, $Re = 10^8$. Values of the boundary layer parameters were estimated from the curves given by Bies, using the above figures.

Since it is desired to apply the empirical results from the present study to the supersonic case, and there are, at present, no reliable in-flight supersonic measurements, the supersonic wind tunnel data of Speaker and Ailman (Reference 11) has been reviewed carefully. This is essentially the sole source of detailed information on the supersonic case once the data of Kistler and Chen (Reference 9) is rejected

(see Section II.1). Figure 4 shows a replot of the Speaker and Ailman data on the present basis. Overall level has been nondimensionalized by dividing by $q/(1 + 0.14\ M^2)$, and the Strouhal number is based on free-stream velocity and boundary layer thickness. The curves have collapsed moderately well, certainly better than the results obtained by using displacement thickness for nondimensionalization, and possibly slightly better than a collapse based on momentum thickness. Curves based on these other parameters are given in Reference 11. Speaker and Ailman also use τ_w for their vertical ordinate collapse, but this change is of little significance, as might be expected from Figure 1.

An empirical curve was sought which, firstly, lay close to the mean empirical curves derived from Bies' results for the flight and wind tunnel cases and, secondly, was a fair representation of the data of Speaker and Ailman for the supersonic cases. The curve shown in Figures 3 and 4 has been chosen. It corresponds to the formula

$$\frac{F(\omega)\,(1 + 0.14\,M^2)^2}{q^2} = \frac{(0.006)^2}{\omega_o \left\{ 1 + (\omega/\omega_o)^2 \right\}^{3/2}}$$

where the typical frequency ω_o has been put equal to $8\ U/\delta$. This curve has the advantage of being analytic, which may simplify theoretical work, and also matches the data well, particularly considering the wide scatter. As can be seen, the curve is probably conservative at the high frequencies for the highest Mach numbers. The large scatter of the data at low frequencies suggests that external effects are occurring, which can not at present be predicted.

There is a definite trend noticeable in Figure 4, which was also pointed out by Speaker and Ailman. The slope of the high frequency portion of the curves for $M > 0.8$ is greater than that of the lower Mach number spectra. Furthermore the curve for $M = 0.42$ agrees closely with that of Bull (Reference 6) in the high frequency region. Typically low Mach number wind tunnel spectra decay at 20 dB per decade at high frequencies, while the present high Mach spectra decay at 40 dB per decade. Little independent data is available to substantiate this trend, although Maestrello's results (Reference 15) taken at $0.63 < M < 0.78$ do show some increase in decay rate. Since the trend to increased rates of decay above a Mach number of about 0.8 cannot be conclusively verified it seems desirable to exercise some caution in making predictions, and this is reflected in the empirical curve in Figure 4. It may be noted that while the empirical curve does lie below the low speed wind tunnel data at high frequencies, it appears to match the subsonic flight data well (see Figure 3). It is thought that the empirical curve may be used with some confidence for aircraft predictions unless extraneous low frequency effects are present.

Use of the above formulae requires a knowledge of boundary layer thickness. The empirical formula suggested by Bies (Reference 10) is recommended

$$\frac{\delta}{x} = 0.37\ Re_x^{-0.2} \left\{ 1 + \left(\frac{Re_x}{2.9 \times 10^7} \right)^2 \right\}^{0.1}$$

where x is the distance from the front of the body and $Re_x = Ux/\nu$ where ν is the kinematic viscosity.

3. CROSS-SPECTRAL DENSITY

The final requirement in determining the characteristics of the fluctuating pressure field is to define the cross-spectral density over the surface. Measurements by many investigators (see Table I) have shown that the cross-spectral density function has the form

$$\phi_{pp}(\xi, \eta, \omega) = A(\xi, \eta, \omega) \cos\left(\frac{\omega \xi}{U_c}\right) \tag{11}$$

where ξ and η are the longitudinal and lateral separations, ω is the circular frequency, and U_c the convection velocity. U_c is also a function of both ξ and ω. For convenience in subsequent mathematics it is usually assumed that the function A is separable so that

$$A(\xi, \eta, \omega) = A_\xi(\xi, \omega)\ A_\eta(\eta, \omega) \tag{12}$$

It is of interest to study the implications of this. Anticipating a future result, both A_ξ and A_η are found to have a negative exponential form, so that

$$A(\xi, \eta, \omega, U_c) = \exp(-a\omega\xi/U_c) \exp(-b\omega\eta/U_c) = \exp(-(a\xi + b\eta)\omega/U_c).$$

Thus, the assumed separable form leads to the prediction that the magnitude of A is constant along straight lines on the surface, forming a diamond pattern surrounding the origin. This characteristic seems physically unreasonable. A more likely form for the lines of constant amplitude would be elliptic corresponding (say) to

$$A(\xi, \eta, \omega, U_c) = \exp - \left[\left\{ (a\xi)^2 + (b\eta)^2 \right\}^{1/2} \omega/U_c \right]$$

The ratio of areas of the two forms is $\pi/2$, suggesting that the usual separable solution underestimates the correlation area by this factor. In fact the lines of constant broadband correlation coefficient usually swell out away from either the lateral or longitudinal directions (References 5 and 11). On the other hand, Bull (Reference 5) and Serafini (Reference 16) have found their results for the amplitude of the narrow-band cross spectrum at an angle to the flow to agree reasonably well

with the separable form, at least at small spacings. Since the use of a separable form provides a distinct analytic simplification for the response calculations, it will be used here. However, in view of the arguments above it is suggested that integrations of the formula containing it be multiplied by a factor $\pi/2$ to allow for its probable underestimate of the correlation area at any frequency.

In the present work the cross power-spectrum is defined following Equations 11 and 12 . Furthermore the function A is nondimensionalized to unity at the origin by dividing by the value of the power spectrum at the relevant frequency. In more general studies the cross power-spectrum would be defined in terms of its amplitude and phase, which are related to the coherence function and convection velocity respectively. However, using the form of Equation 11 introduces the convection velocity simply as a nondimensionalizing parameter.

a. Convection Velocity

The convection velocity is found to be a function of both frequency and spatial separation. This variation with frequency is due to the varying speed of the different size eddies in the boundary layer. The variation with spatial separation is thought to be due primarily to the typical accelerated eddy trajectories in the boundary layer (Reference 5) together with the effects of the varying coherence lengths of eddies moving at different speeds (Reference 6).

There are many problems even in defining a proper convection velocity (Reference 17) but the definition used here will be based on methods commonly used in deriving the data; that is, the convection velocity is given by dividing the spacing of two locations by the time delay required to give maximum narrow-band correlation of the signals from the locations. Bull (Reference 5) gives a complete discussion.

Although results on convection velocity from one boundary layer tend to be consistent, results from different workers do tend to differ. The results of Bull (Reference 5) have been used to generate a set of empirical curves, and these are compared to other results. We have no way of knowing which set of results will be more realistic in the flight case.

Empirical curves through Bull's data are shown in Figures 5 and 6. They correspond to formula

$$\frac{U_c}{U_o} = 0.075 + 0.3 \exp\left(-0.11 \frac{\omega \delta}{U_o}\right) - 0.25 \exp\left(-1.2 \xi/\delta\right)$$

where the broadband convection velocity curves correspond to $\omega \delta/U_o = 8$, giving

$$\frac{U_c}{U_o} = 0.8 - 0.25 \exp(-1.2\ \xi/\delta)$$

An alternative empirical curve based on Bies' empirical formula for the effect of frequency (Reference 10) corresponds to

$$\frac{U_c}{U_o} = \left\{0.8 - 0.25 \exp(-1.2\ \xi/\delta)\right\}\left(\frac{8\ U_o}{\omega\ \delta}\right)^{0.09}$$

This reduces to Bies' formula, which ignores spacing, at $\xi/\delta = 0.75$.

The present empirical curves fit Bull's data quite well at longitudinal spacings less than about two boundary layer thicknesses, but may be somewhat low at the very highest spacings. This will not usually be significant as all but the lowest frequency components will have lost all coherence at high spacings. It should be noted that no attempt has been made to integrate the empirical curve over the spectrum to derive a broadband result, but it is assumed that the results of such a procedure would give a reasonable result since the result at the maximum power point is consistent.

In Figure 5 the present empirical curve for broadband convection velocity is compared with results from other investigators. It has been usual to nondimensionalize the spacing (ξ) by dividing by the displacement thickness (δ^*). In the present work, boundary layer thickness (δ) has been used. This is consistent with the rest of the report, but also corresponds to the dimension of the largest eddies, a physical scale which would be expected to be important. Comparison of the two scale parameters does not show either to be plainly better. Speaker and Ailman's supersonic data (Reference 11) agrees better with that of Bull (Reference 5) under the present scheme, but better with that of Willmarth and Wooldridge (Reference 18) and Serafini (Reference 16) using the δ^* scheme. The scatter apparent in Figure 5 shows that the physical features underlying convection velocity are not known at present.

One important conclusion may be drawn from Figure 5. The typical eddy convection speed in a boundary layer is often quoted as being 0.8 of the free stream velocity. This is the asymptotic value at large spacings and refers essentially to the low frequency components in the flow. In particular, this value does not refer to the typical convection velocity of eddies past a single microphone. This latter velocity is given by the asymptotic value of the convection velocity at zero spacing. The typical value of this is about $0.5\ U_o$, and this is the value which should be used in correction of microphone size effects and similar calculations (References 19 - 22). The predicted value of microphone correction is very sensitive to small changes of convection velocity. Careful experiments using very small microphones to determine the asymptotic value of convection velocity as a function of frequency seem very worthwhile. It should be noted that the various authors applied their own correction

for microphone size and no further adjustment has been made for data presented in this report.

Kistler and Chen (Reference 9) presented data indicating that the broadband convection velocity was a function of Mach number. A new plot of their data is also shown on Figure 5. It will be noted that their data was taken at very low values of spacing (ξ) to boundary layer thickness (δ), and that, within the scatter, it is completely consistent with the subsonic data. Indeed Kistler and Chen took several results at different spacings at the same Mach number and found the predicted rise in convection velocity with increasing ξ/δ in the majority of cases. It may also be noted that their flat plate data, taken under a thinner boundary layer (not plotted on their original curve), is also consistent with the present trend. It is concluded that the effect of Mach number on convection velocity given by Kistler and Chen is spurious and results from the increasingly thin boundary layer used in their high Mach number experiments. Thus, the present empirical curves for convection velocity are thought to apply equally well at high and low Mach numbers.

Speaker and Ailman's results (Reference 11) for a supersonic case were shown on Figure 5. In fact the graph of τ_{opt} versus ξ given in their report suggests that the value of U_c/U_o at large spacings would be about 0.95. This would be consistent with the physical picture that the outer parts of the boundary layer, moving supersonically with respect to the wall, would be more significant at supersonic speeds. Since there is no further data to substantiate this point the effect has not been included here, but it seems worthy of further research.

Inclusion of these convection velocity effects in response calculations is difficult, and will probably require computer evaluation of the joint acceptance. It seems very desirable to perform such computations to evaluate the effect of convection velocity, and to derive simplified methods of including its variation in response studies.

b. Empirical Determination of Cross-Spectral Density

If a separable form for the cross-spectral density is assumed (see Section II.3.) then

$$\Phi_{pp} = \Phi_\xi \Phi_\eta = \left\{ A_\xi \cos\left(\frac{\omega \xi}{U_c}\right)\right\} A_\eta$$

and we need to determine Φ_ξ and Φ_η separately.

The early workers (References 13, 18) used a narrow band correlation at zero time delay to determine the longitudinal and lateral cross spectra, and found that the longitudinal cross spectrum corresponded to

$$\phi_\xi = A_\xi \left(\frac{\omega \xi}{U_c}\right) \cos \left(\frac{\omega \xi}{U_c}\right)$$

Thus, the cross spectra were found to collapse on a Strouhal number based on spacing and convection velocity. Also it was found

$$\phi_\eta = A_\eta \left(\frac{\omega \eta}{U_c}\right)$$

although there is no real basis, other than convenience, for introducing U_c in the denominator here. Accurate determination of $A_\xi (\omega \xi/U_c)$ is only possible when $\cos (\omega \xi/U_c)$ is near unity. Furthermore the use of non-ideal filters can cause errors. Consequently, Bull (Reference 6) and Corcos (Reference 23) proposed to measure the value of A_ξ from the maximum amplitude of the narrow-band space-time correlations and showed that this introduced no error into the result, even using non-ideal filters. Note that A_ξ is the amplitude of the cross-spectral density and is also known as the coherence function, although sometimes the square of this amplitude is referred to as the coherence function.

The most complete results to date were taken by Bull, and are shown in Figure 7. Other workers had recognized that the assumption that the amplitude of the cross spectrum was a function only of $(\omega \xi/U_c)$ must break down at the lowest frequencies since very large correlation lengths would be implied. Bull's data showed that this was indeed true and that the low frequency curves fell off comparatively faster. Alternatively this same effect may be observed on the curves of constant ξ in the data which do not tend to unity for large ξ. The effect is due to the finite thickness of the boundary layer. Bull found that the lower frequency eddies lost coherence essentially as a group, in a way which was not a function of frequency.

Many workers have observed that the functional form of the amplitude broadband or narrow-band correlation curves can be represented well by a negative exponential. A theoretical justification of this is presented in the Appendix. Bull gives the following approximation for his data at high frequencies

$$\left| A_\xi \right| = \exp \left(-0.1\, \omega \xi/U_c\right) \qquad (13)$$

In addition Bull gives results showing that the asymptotic value of his curves for constant ξ is given by

$$\left|A_\xi\right|_{\omega \to 0} = \exp \left(-0.27\, \xi/\delta\right) \qquad (14)$$

An empirical formula which seems to match the complete data well is

$$|(A_\xi)| = \exp\left[-\left\{(0.1\,\omega\xi/U_c)^2 + (0.27\,\xi/\delta)^2\right\}^{0.5}\right] \qquad (15)$$

This is shown in Figure 7.

An alternative method is to use formula 13 for $(\omega\,\delta/U_c) > 2.7$ and formula 14 for $\omega\,\delta/U_c < 2.7$. This will tend to overestimate the correlations between, roughly, $2 < \omega\delta/U_c < 8$, but is simpler to apply. Note that in the present case the overestimate referred to above is balanced by an underestimate of the overall curve (see Figure 7) so the total error is expected to be small. Bull's data is the only evidence available on the low frequency cross-spectral effects. However, many investigators have reported higher frequency data. Table I gives a listing of the results, and gives the typical value of the constant in the negative experimental data required to put a curve of this form through their data. Study of Table I suggests that the value of 0.1 in the longitudinal negative exponent may be slightly low. However, no change has been made in the present formulae.

The form of the lateral cross-spectral density is found to be a simple decay curve. Bull's data corresponds well to the curve

$$A_\eta = \exp(-0.72\,\omega\eta/U_c) \qquad (16)$$

As in the longitudinal case, the low frequency results show a faster decay, and the asymptotic form for the lateral case corresponds approximately to

$$A_\eta = \exp(-1.95\,\eta/\delta) \qquad (17)$$

It should be noted that this form somewhat underestimates the values at the largest spacings compared to Bull's results, but it does correspond to the same criterion $\omega\,\delta/U_c = 2.7$ as the longitudinal case. This is consistent with the physical picture that the same group of eddies in the boundary layer are responsible for the departure from both longitudinal and lateral Strouhal similarity of the cross spectra. A form similar to (15) could be used for the lateral cross spectra but, for simplicity, the use of Equations 16 and 17 above and below $\omega\,\delta/U_c = 2.7$ respectively is recommended.

Table I also shows the results of fitting exponential curves to the lateral cross spectra of other workers. There is rather more scatter in the results here, but there seems to be no justification in changing the value of the exponent derived from Bull's data in a typical case. Additional comments relevant to this point are made in the following section.

SECTION III

NONEQUILIBRIUM BOUNDARY LAYERS

The empirical formulae given in the preceding section refer to the pressure fluctuations occurring beneath an equilibrium boundary layer, that is, one which is fully established at a sufficiently high Reynolds number, and is unperturbed by effects such as pressure gradients or protuberances. In most modern aircraft designs the boundary layer should be near the equilibrium condition over much of the cabin, but invariably non-equilibrium boundary layers will be encountered.

The only published work on the effects of pressure gradient is due to Schloemer (Reference 4) and even his results were taken only for a single favorable and a single unfavorable pressure gradient. As might be expected the favorable pressure gradient reduced, and the unfavorable increased, the intensity of the pressure fluctuations. The direct effect of pressure gradient is to increase both low and high frequency components for the unfavorable case, and to substantially reduce the low frequency component while increasing the high for the favorable case. This latter effect is essentially due to the thinner boundary layer for the favorable pressure gradient. Comparing the spectra using a Strouhal number based on actual boundary layer thickness shows that the low Strouhal number components (<0.3) are increased by about 5 dB for the unfavorable pressure gradient and reduced by the same amount for the favorable case. However, at the higher Strouhal numbers (>5.0) both favorable and unfavorable pressure gradients showed a reduction in intensity compared to the equilibrium values.

It is extremely difficult to find a single "figure of merit" for a given pressure gradient, and even if this could be defined there is not sufficient data to define the effects of this on pressure fluctuations. The general discussion above indicates the complexity of the problems, and represents the state of knowledge at the present time. Physically one might also expect variations in correlation area in non-equilibrium flow, although Schloemer's data shows little effect, at least at the higher frequencies (See Table I).

It is equally difficult to define in any general way the effects of protuberances or roughness on the pressure fluctuations. It is found that the protuberances do add intensity at the low frequencies up to 20 dB at a Strouhal number near unity. Data on this was given by Jorgensen (Reference 24) and by Willmarth and Wooldridge (Reference 3). Again definition of a single roughness parameter and correlation of this with the pressure fluctuations is not, at present, feasible.

Efforts were made during the present work to correlate the frequency spectra with the physical picture of the wall and wake boundary layer components advanced by Coles (Reference 25). This is attractive since the wall component would be expected to give rise to the high frequencies while the wake component generated the low frequencies. Some success was achieved with this approach, but not enough data is available to allow numerical predictions to be made.

An alternative physical picture of these effects is provided by the hypothesis that periodic eruptions of the wall layer are responsible for the major part of the observed pressure field (References 5, 12). Recently Shraub and Kline (Reference 26) have studied the effects of pressure gradient on the eruption mechanism. Their data is somewhat scattered, but they do show a cessation of the eruption process for a sufficiently favorable pressure gradient. This would suggest that the high frequency components of the pressure fluctuation would be markedly reduced under these conditions. It seems that a study of the pressure fluctuations under systematically varied nonequilibrium boundary layers could provide valuable information which would enable improved predictions to be made.

Perturbed supersonic flow gives rise to very many additional problems such as the effects of separated flow and oscillating shocks, or of shock-turbulence interaction. Complete examination of these effects requires a separate report. Methods for predicting the gross features of the fluctuation pressure beneath various flows are given in Reference 27, while data on the effects of typical aircraft type protuberances are given in References 11 and 28.

SECTION IV

CONCLUSIONS

The pressure fluctuations occurring beneath equilibrium boundary layers at subsonic and supersonic speeds have been reviewed. Empirical formulae have been put forward to describe the intensity, spectra, and cross spectra of the fluctuations. These formulae are sufficient to define the statistical characteristics of the fluctuating pressures required for structural response calculations. The objectives of the empirical methods were: (1) simplicity, (2) relation to the physical parameters of the flow and (3) good agreement with the available data. It is thought that each of these objectives has been acheived. The formulae are summarized below.

Intensity

$$p_{rms}/q = 0.006/(1 + 0.14\ M^2)$$

Spectrum

$$\frac{p^2(\omega)}{q^2} = \left\{ \frac{0.006}{1 + 0.14\ M^2} \right\}^2 \frac{1}{\omega_o \left(1 + \omega^2/\omega_o^2\right)^{3/2}}$$

where

$$\omega_o = 8\ U/\delta\ ,\ \frac{\delta}{x} = 0.37\ Re_x^{-0.2} \left\{ 1 + \left(\frac{Re_x}{0.9 \times 10^7} \right)^2 \right\}^{0.1}$$

Cross Spectrum

$$\phi_{pp}(\xi, \eta, \omega) = \pi/2\ \phi_\xi(\xi, \omega)\ \phi_\eta(\eta, \omega)$$

where

$$\phi_\xi(\xi, \omega) = \exp(-0.1\ \omega\ \xi/U_c) \cos(\omega\ \xi/U_c),\ \omega\delta/U_c > 2.7$$

$$= \exp(-0.27\ \xi/\delta) \cos(\omega\ \xi/U_c),\ \omega\delta/U_c < 2.7$$

$$\phi_\eta(\eta, \omega) = \exp(-0.72\ \omega\ \eta/U_c),\ \omega\ \delta/U_c > 2.7$$

$$= \exp(-1.95\ \eta/\delta),\ \omega\delta/U_c < 2.7$$

Convection Velocity

$$\frac{U_c}{U_o} = 0.075 + 0.3 \exp\left(-0.11 \frac{\omega \delta}{U_o}\right) - 0.25 \exp\left(\frac{-1.2\xi}{\delta}\right)$$

Several alternative forms for these formulae are given in the text.

The following conclusions have also been drawn as a result of the present work:

1. The change in fluctuation level with Mach number may be attributed directly to the reduced density of the wall layer.

2. Compressibility ($M > 0.8$) seems to increase the rate of decay of the high frequency part of the fluctuating pressure spectrum. (These facts have not been accounted for in the present formulae).

3. Convection velocity is not a direct function of Mach number.

4. Use of an exponentially decaying correlation or coherence function seems to have theoretical justification at large spacings (see the Appendix).

5. Separation of variables in the cross spectrum function leads to physically unreasonable results.

The use of the above results in structural response calculations should be comparatively straightforward, except for the convection velocity term. The variation of convection velocity with spacing does complicate joint acceptance calculation. It is recommended that joint acceptance results be computed with convection velocity as a function of spacing to determine the significance of the effect in structural response.

The results are probably reliable at subsonic speeds but are based on very limited data for supersonic or non-equilibrium boundary layers. Further sources of data are urgently required, but at the present time the formulae given represent the best available estimate.

REFERENCES

1. K. McK Eldred, W. Roberts, and R. W. White, Structural Vibrations in Space Vehicles, WADD TR 61-62, December 1961.

2. G. M. Lilley, Pressure Fluctuations in an Incompressible Turbulent Boundary Layer, C of A Rep. 133, 1960.

3. W. W. Willmarth, "Corrigendum: Measurements of the Fluctuating Pressure at the Wall Beneath a Thick Turbulent Boundary Layer," J. Fluid Mech., Vol. 21, Pt. 1, pp. 107-109, January 1965.

4. H. H. Schloemer, "Effects of Pressure Gradients on Turbulent-Boundary-Layer Wall-Pressure Fluctuations," J. Acoust. Soc. Am., Vol. 42, pp. 93-113, July 1967.

5. M. V. Lowson, Pressure Fluctuations in Turbulent Boundary Layers," NASA TN D-3156, December 1965.

6. M. K. Bull, Properties of the Fluctuating Wall Pressure Field of a Turbulent Boundary Layer, AGARD Rep 455, April 1963.

7. M. V. Morkovin, "Effects of Compressibility on Turbulent Flows," p. 367 of Mecanique de la Turbulence, CRNS, 1962.

8. A. H. Shapiro, The Dynamics and Thermodynamics of Compressible Fluid Flow, Ronald Press, New York, 1954.

9. A. L. Kistler, and W. S. Chen, The Fluctuating Pressure Field in a Supersonic Turbulent Boundary Layer, Jet Propulsion Laboratory Technical Report, No. 32-277, August 1962.

10. D. W. Bies, A Review of Flight and Wind Tunnel Measurements of Boundary Layer Pressure Fluctuations and Induced Structural Response, NASA CR 626, 1966.

11. W. V. Speaker, and C. M. Ailman, Spectra and Space-Time Correlations of the Fluctuating Pressures at a Wall Beneath a Supersonic Turbulent Boundary Layer Perturbed by Steps and Shock Waves, NASA CR 486, 1966.

12. T. J. Black, "Some Practical Applications of a New Theory of Wall Turbulence," Proc. Heat Trans. and Fluid Mech. Inst., pp. 366-380, 1966.

13. T. H. Hodgson, Pressure Fluctuations in Shear Flow Turbulence, Ph.D. Thesis, University of London, 1962.

14. J. S. Gibson, Boundary Layer Noise Measurements on a Large Turbofan Aircraft, Paper I 10, 70th Meeting of the Acoust. Soc. of Am., November 1965.

15. L. Maestrello, Boundary Layer Pressure Fluctuations on the 707 Prototype Airplane, Paper at 64th Meeting Acoust. Soc. Am., November 1962.

16. J. S. Serafini, Wall Pressure Fluctuations and Pressure Velocity Correlations in a Turbulent Boundary Layer, NASA TR R-165, December 1963.

17. J. A. B. Wills, On Pressure Fluctuations Under Turbulent Boundary Layers, N.P.L. (England) Aero Rep. 1131, December 1961.

18. W. W. Willmarth, and C. E. Wooldridge, "Measurements of the Fluctuating Pressure at the Wall Beneath a Thick Turbulent Boundary Layer," J. Fluid Mech., Vol. 14, pp. 187-210, 1962.

19. G. M. Corcos, "Resolutions of Pressure in Turbulence," J. Acoust. Soc. Am., Vol. 35, No. 2, pp. 192-199, February 1963.

20. W. W. Willmarth, and F. W. Roos, "Resolution and Structure of the Wall Pressure Field Beneath a Turbulent Boundary Layer," J. Fluid Mech., Vol. 22, Part I, pp. 81-94, 1965.

21. K. L. Chandiramani, Interpretation of Wall Pressure Measurements Under a Turbulent Boundary Layer, Bolt, Beranek and Newman, Inc., Report No. 1310, August 1965.

22. P. H. White, "Effect of Transducer Size, Shape, and Surface Sensitivity on the Measurement of Boundary Layer Pressures," J. Acoust. Soc. Am., Vol. 41, pp. 558-1363, May 1967.

23. G. M. Corcos, "The Structure of the Turbulent Pressure Field in Boundary Layer Flows," J. Fluid Mech., Vol. 18, p. 353, 1964.

24. D. W. Jorgensen, Measurements of Fluctuating Pressures on a Wall Adjacent to a Turbulent Boundary Layer, DTMB Rep. 1744, 1963.

25. D. W. Coles, "The Law of the Wake in the Turbulent Boundary Layer," J. Fluid Mech., Vol. 1, pp. 191-226, 1956.

26. F. A. Shraub, and S. J. Kline, A Study of the Structure of the Turbulent Boundary Layer With and Without Longitudinal Pressure Gradients, Stanford University, Dept. Mech. Eng., Rep. MD-12, 1965.

27. M. V. Lowson, Prediction of the Inflight Fluctuating Pressure on Space Vehicles, Wyle Research Staff Report WR 65-26, December 1965.

28. J. S. Murphy, et al., Wind Tunnel Investigation of Turbulent Boundary Layer Noise as Related to Design Criteria for High Performance Vehicles, NASA TN-D2247, April 1964.

29. J. W. Priestley, Correlation Studies of Pressure Fluctuation on the Ground Beneath a Turbulent Boundary Layer, N.B.S. Rep. 8942, July 1966.

30. J. S. Bendat, Principles and Applications of Random Noise Theory, Wiley and Sons, New York, 1958.

31. H. P. Bakewell, et al., Wall Pressure Correlation in Turbulent Pipe Flow, U. S. Navy Sound Lab., Rep. 4559, August 1962.

32. R. D. Shattuck, Sound Pressures and Correlations of Noise on the Fuselage of a Jet Aircraft in Flight, NASA TN-D-1086, August 1961.

33. D. J. M. Williams, Measurements of the Surface Pressure Fluctuations in a Turbulent Boundary Layer in Air at Supersonic Speeds, University of Southampton, AASU Rep. 162, December 1960.

34. P. M. Belcher, Predictions of Boundary-Layer Turbulence Spectra and Correlations for Supersonic Flight, Presented at the 5th International Acoustical Congress, Liege, Belgium, September 1965.

APPENDIX

THE BOUNDARY LAYER AS A MARKOV PROCESS

It is of interest to attempt to describe the correlation functions using theoretical arguments. Those presented below are based on work by Priestley (Reference 29).

Consider signals x_1, x_2, x_3 recorded at three points spaced ξ apart as shown

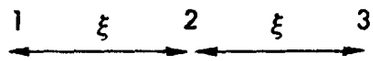

Assume a homogeneous stationary process so that we can define

$$\frac{\overline{x_1 x_2}}{\overline{x_1^2}} = \frac{\overline{x_2 x_3}}{\overline{x_2^2}} = R(\xi), \text{ also } \frac{\overline{x_1 x_3}}{\overline{x_1^2}} = R(2\xi)$$

Also define

$$x_2 = R(\xi)\, x_1 + x_{21}$$

so that x_{21} is the part of x_2 which is uncorrelated with x_1. Similarly, put

$$x_3 = R(\xi)\, x_2 + x_{32}$$

and

$$x_3 = R(2\xi)\, x_1 + x_{31}$$

combining these equations

$$R(2\xi)\, x_1 + x_{31} = R^2(\xi)\, x_1 + R(\xi)\, x_{21} + x_{32}$$

Multiplying through by x_1 and taking means

$$R(2\xi) = R^2(\xi) + \overline{x_{32} x_1} / x_1^2$$

where the remaining double suffix terms drop out because they are uncorrelated with x_1. If $\overline{x_{32} x_1} = 0$ (together with similar terms) then the process may be repeated indefinitely for successive stations giving

$$R(n\xi) = R^n(\xi)$$

The solution to this functional equation can be shown to be

$$R(\xi) = \exp(a\xi)$$

where a is a negative number in order for the correlation to reach a maximum at zero.

In fact, if $\overline{x_{32}\, x_1}$ etc., $= 0$ then the process is a Markov chain and the negative exponential correlation function form has been proved by other writers in a rigorous manner (Reference 30).

Thus we predict an exponential decay for the amplitude of the broad-band or narrow-band spatial correlation unless there is some mechanism by which pressure patterns at 1 can be recorded at 3 without passing 2. This would be the case if coherent paiterns were carried around by an eddy so that they were close to 3 but away from 2. This will tend not to occur for large spacings and high frequencies, but may occur at small spacings and low frequencies.

Thus it appears that there is theoretical justification for assuming an exponential form for the amplitude of correlation functions for boundary layer pressure fluctuations at large spacings. The arguments also show how the exponential form could not be expected to apply at small spacings.

TABLE I

CROSS POWER SPECTRA FROM VARIOUS SOURCES

Note: Numbers given are approximate negative exponential coefficients required to fit the data. Since an exponential curve is not usually an exact fit the numbers given are accurate at best to about ± 10 percent in general.

Investigator	Longitudinal Cross PSD	Lateral Cross PSD	Remarks
Bull (6)	0.1	0.72	M = 0.3 and 0.5
Willmarth and Wooldridge (18)	0.11 0.11	0.7 0.5	$\omega\delta^*/U_o \sim 0.62$ $\omega\delta^*/U_o^o \sim 5.3$
Bakewell (31)	0.11		
Maestrello (15)	0.1	1.5	
Schloemer (4)	0.11 0.1 0.15	0.9 0.9 0.8	Zero Pressure Gradient Favorable Pressure Gradient Adverse Pressure Gradient
Hodgson (13)	0.14		Small Wind Tunnel
Shattuck (32)	0.11		Based on 400 cps at M = 0.81. Other measurements adversely affected by engine noise or microphone resolution.
Jorgensen (24)	0.14 0.19 0.22		U_o^o = 50 fps U_o^o = 100 fps U_o^o = 200 fps } Based on 1st Peak
		$1.3 \times U_c/U_o^o$ $2.0 \times U_c/U_o^o$	$\omega\eta/U_o^o = 2.8$ $\omega\eta/U_o^o = 0.63$
Priestley (29)	0.25		Typical Atmospheric Boundary Layer

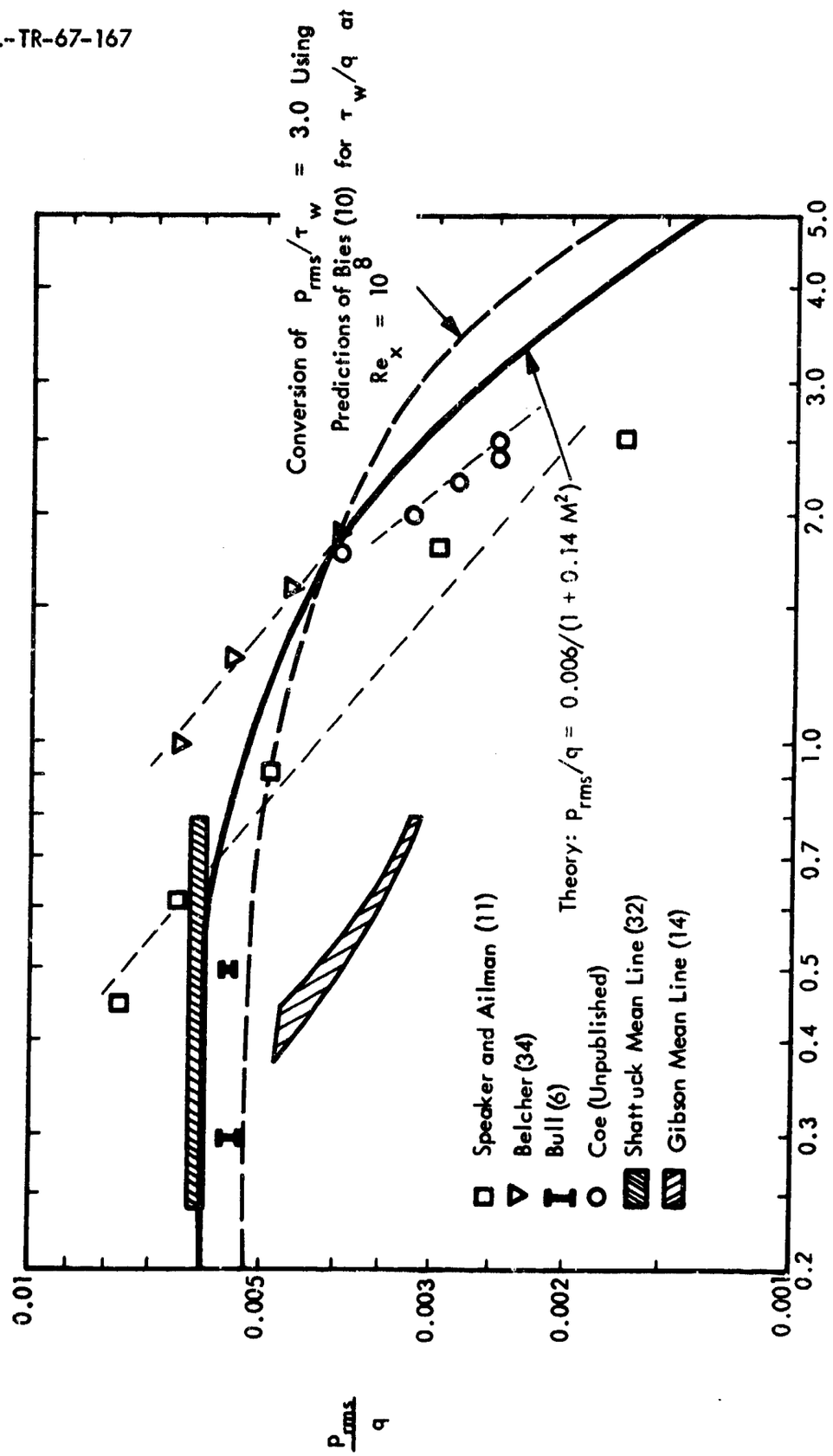

Figure 1a. Fluctuating Pressure Nondimensionalized by Dynamic Head versus Mach Number

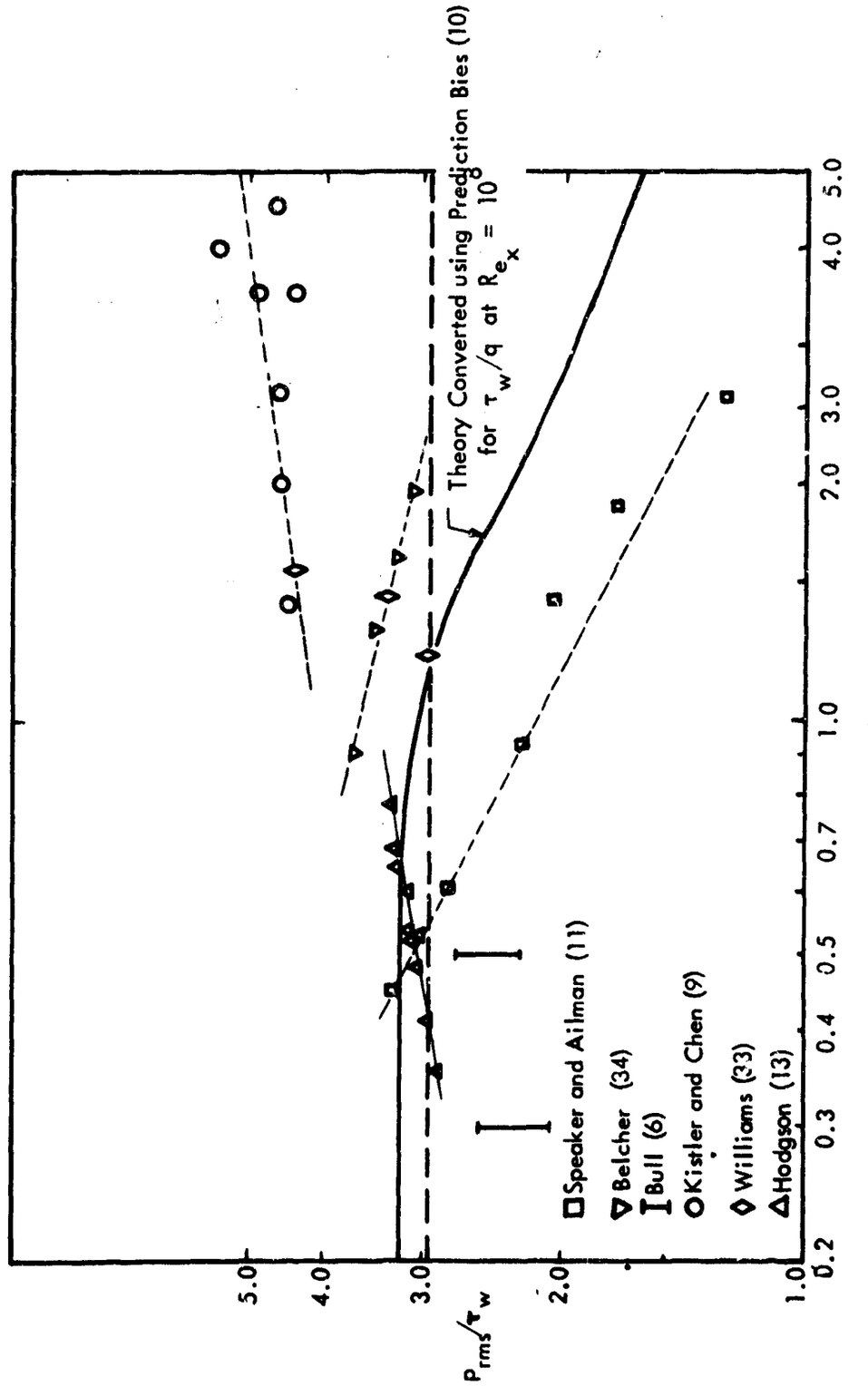

Figure 1b. Fluctuating Pressure Nondimensionalized by Wall Shear Stress versus Mach Number

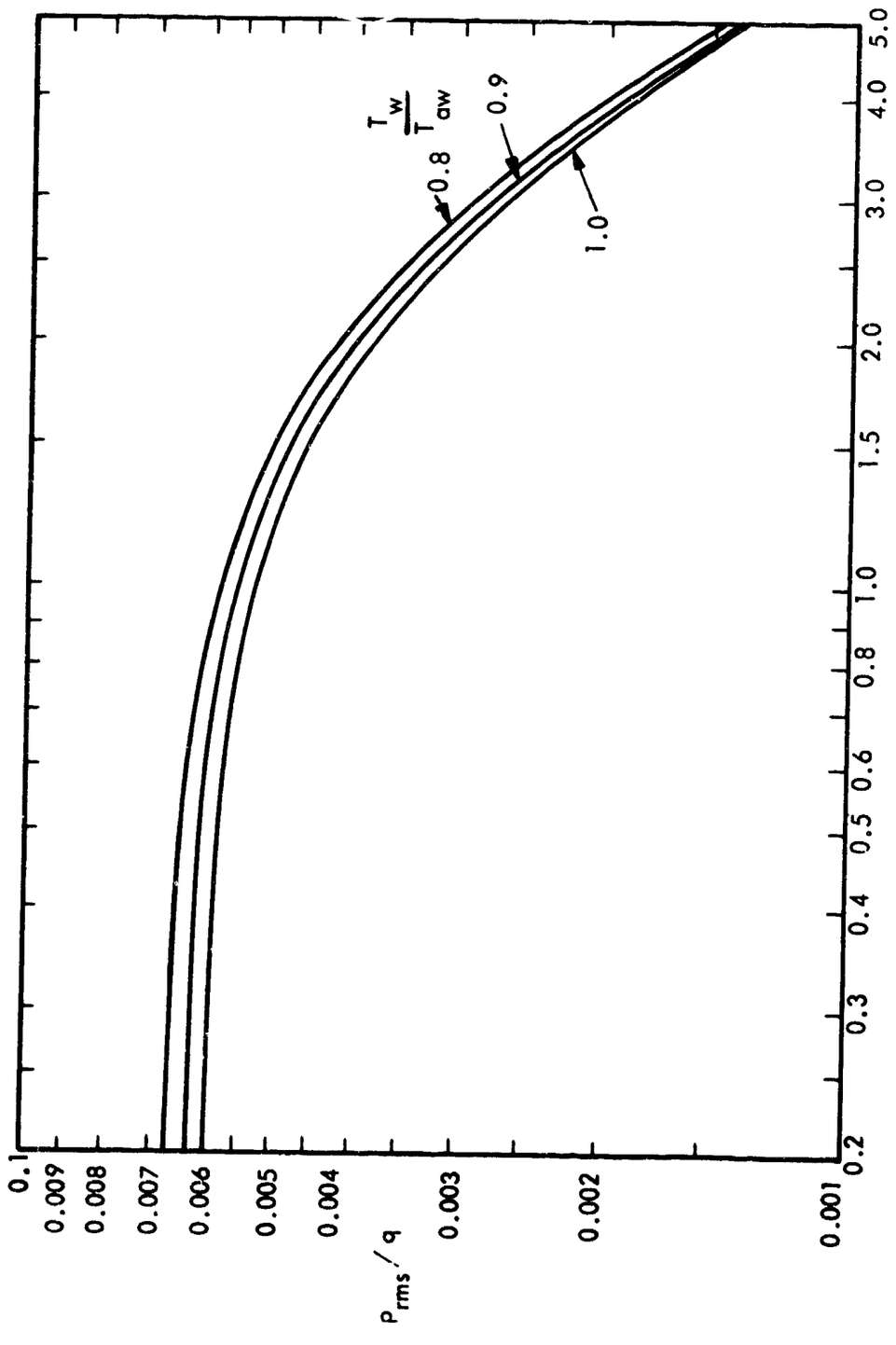

Figure 2. Effect of Wall Temperature on Fluctuating Pressures

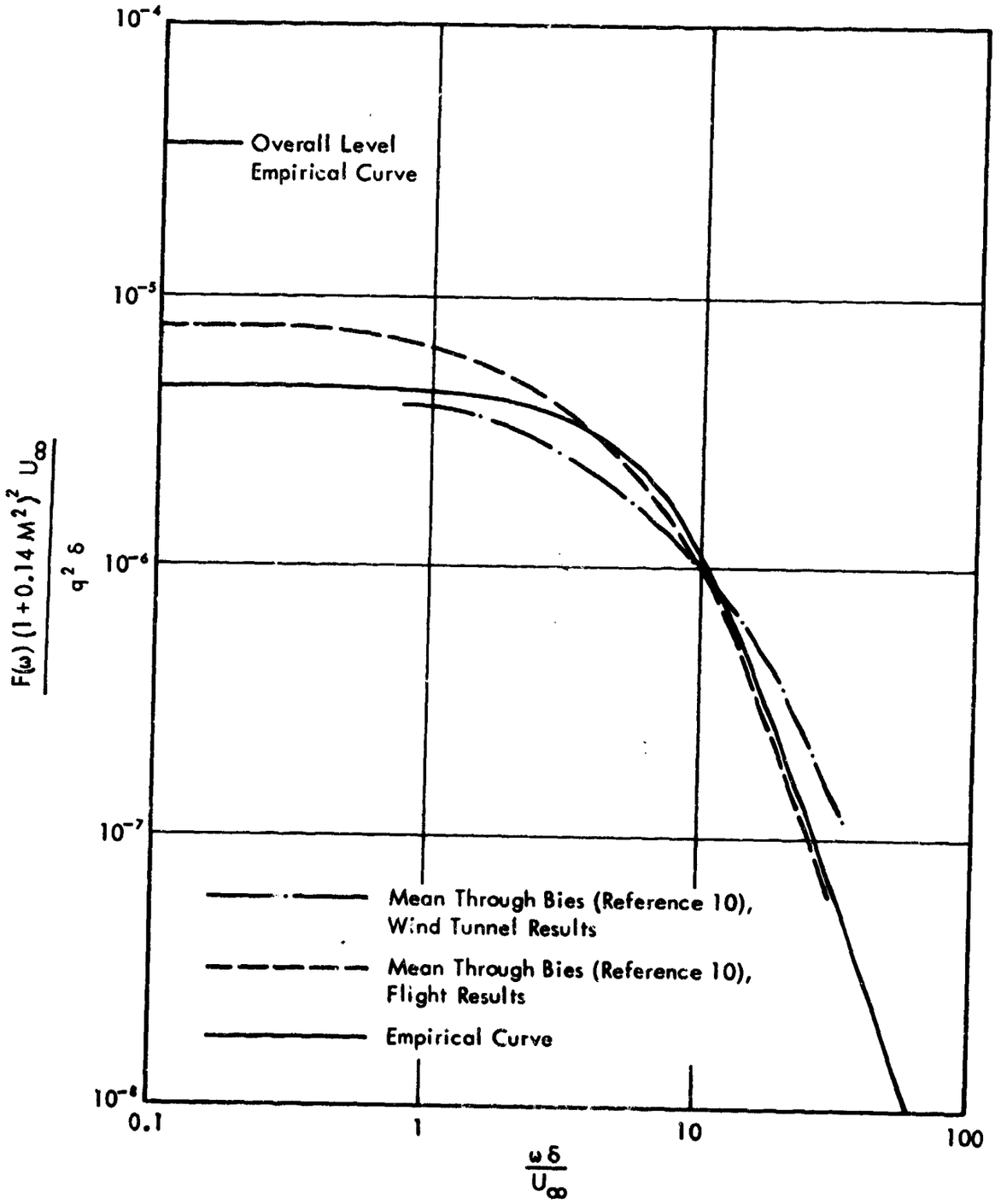

Figure 3. Comparison of Empirical Curve with Data from Bies (Reference 10)

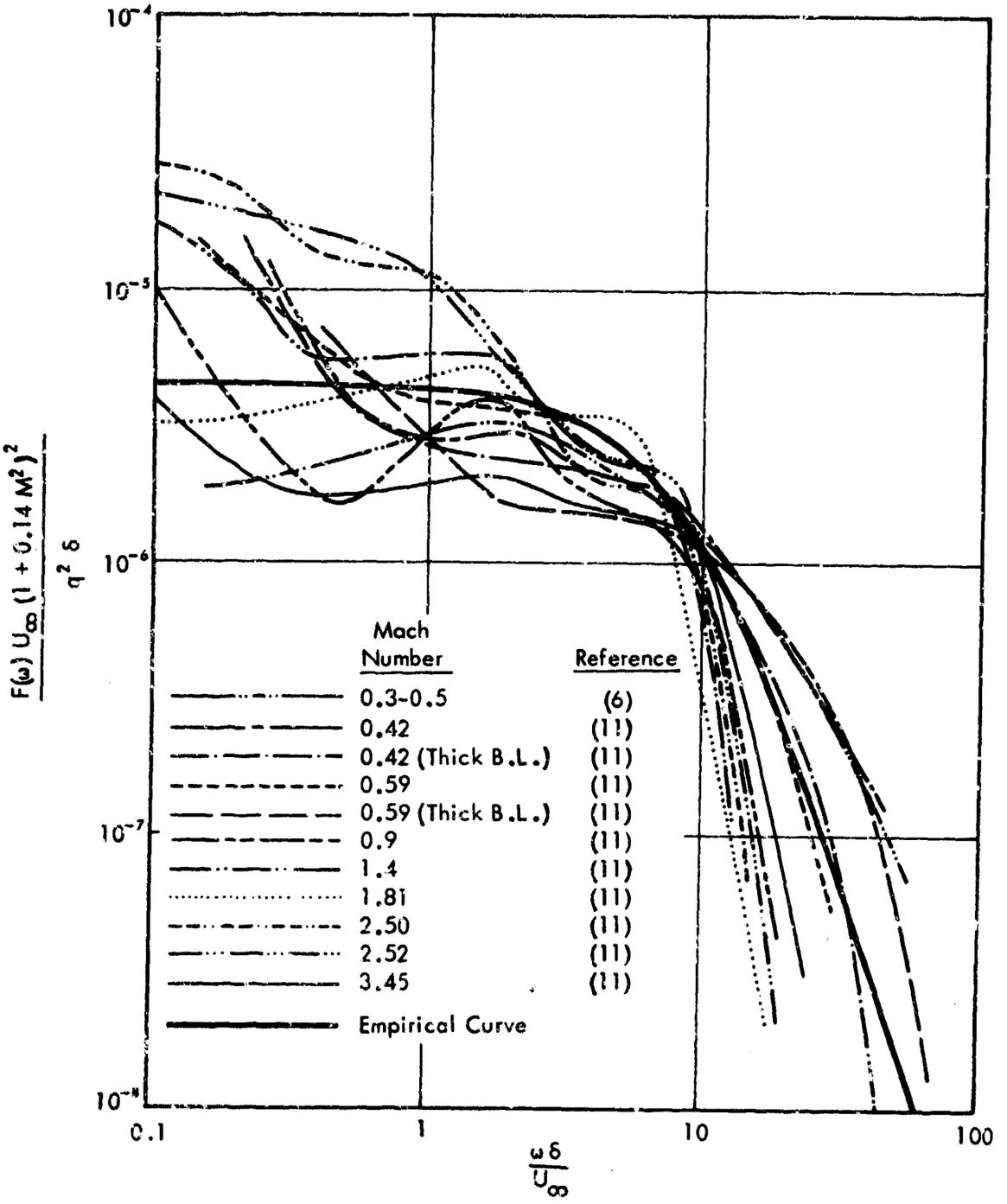

Figure 4. Comparison of Pressure Fluctuation Spectra

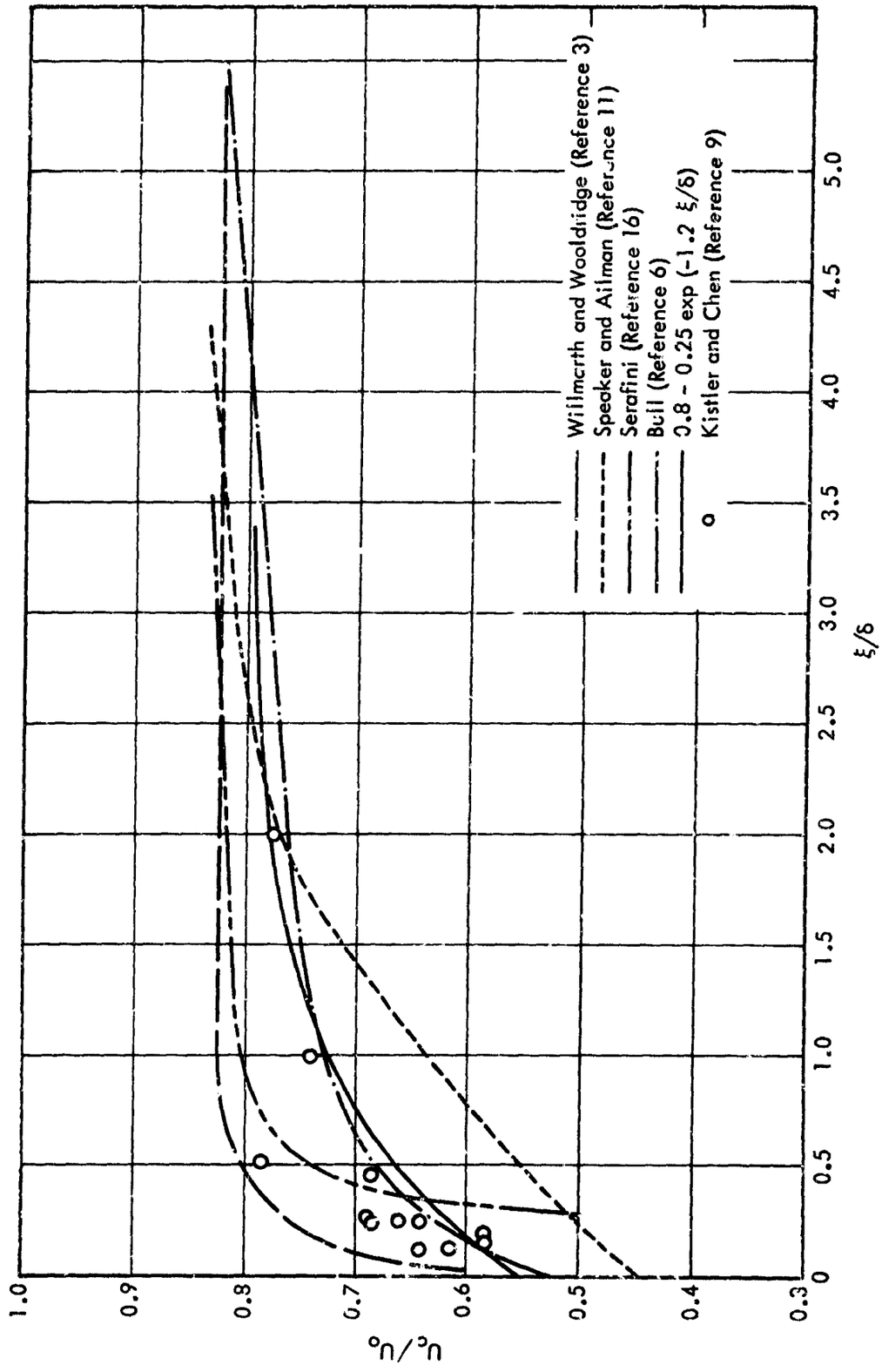

Figure 5. Overall Convection Velocity Versus Spacing

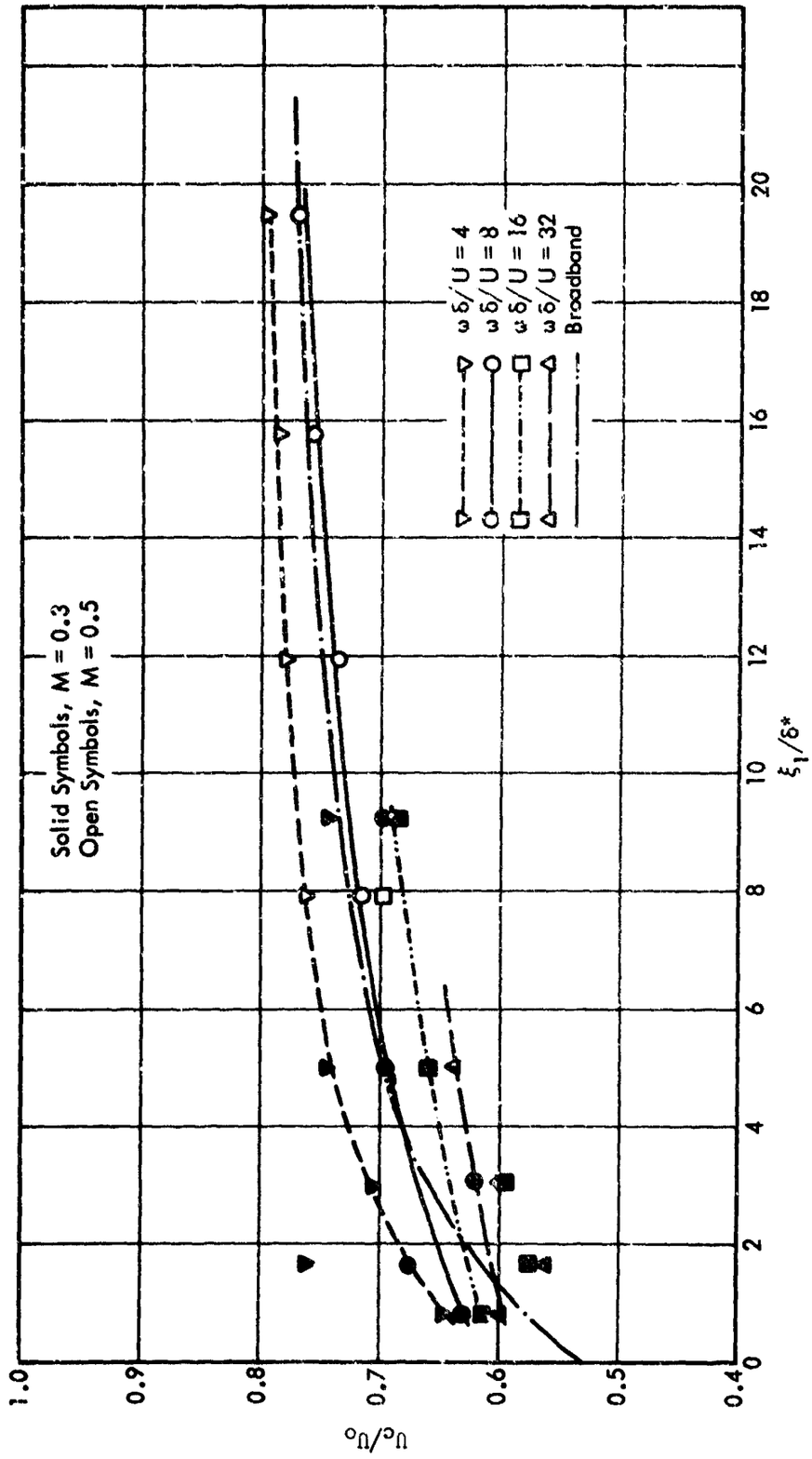

Figure 6. Narrow-Band Convection Velocities - Cross Plot from Bull (Reference 6)

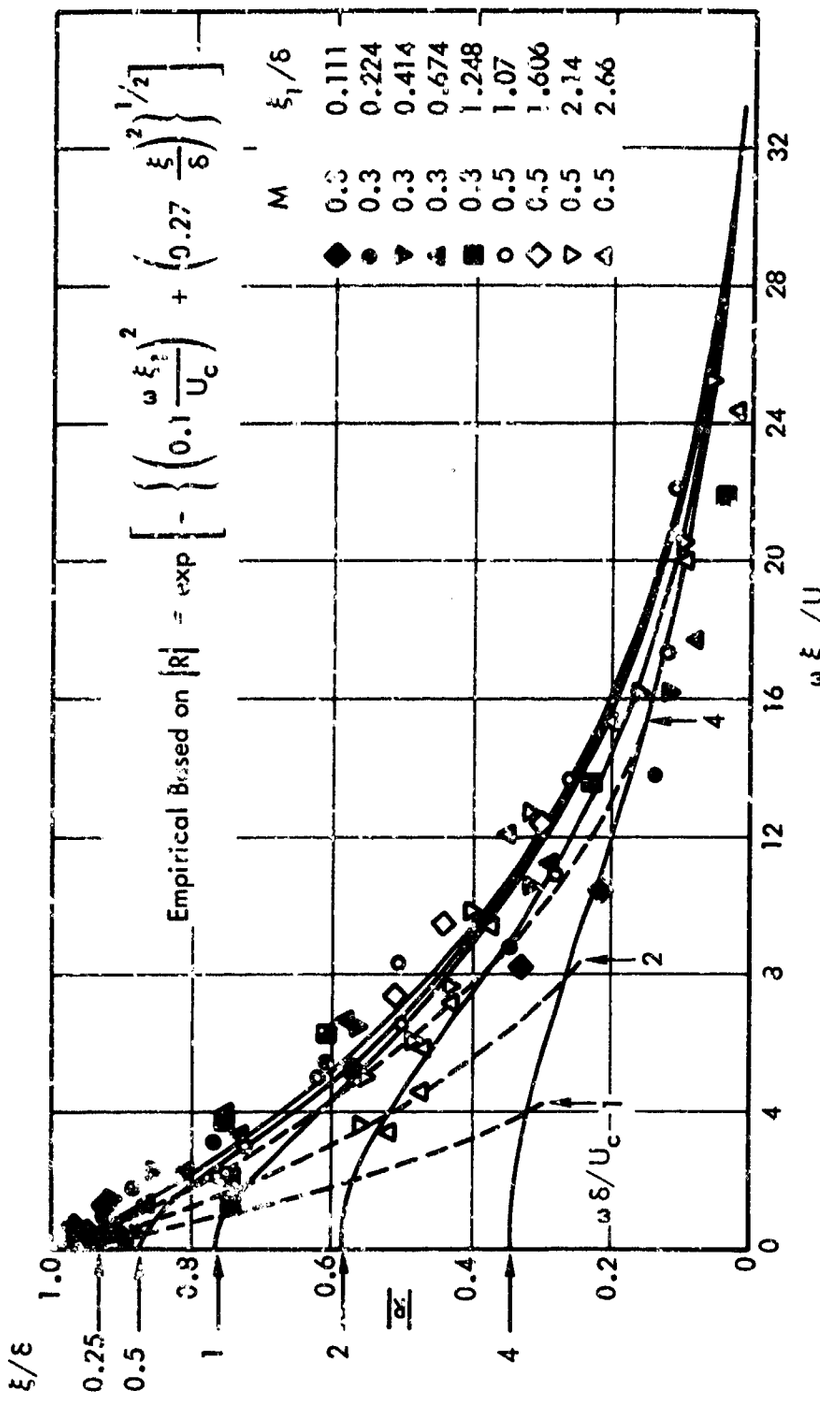

Figure 7. Amplitude of Longitudinal Cross Power-Spectrum Data from Bull (Reference 6)

Unclassified

Security Classification

DOCUMENT CONTROL DATA - R&D

(Security classification of title, body of abstract and indexing annotation must be entered when the overall report is classified)

1. ORIGINATING ACTIVITY (Corporate author) Wyle Laboratories 7800 Governors Drive W. Huntsville, Alabama 35800	2a. REPORT SECURITY CLASSIFICATION Unclassified 2b. GROUP N/A

3. REPORT TITLE

Prediction of Boundary Layer Pressure Fluctuations

4. DESCRIPTIVE NOTES (Type of report and inclusive dates)

Research Staff Report January -- October 1967

5. AUTHOR(S) (Last name, first name, initial)

Lowson, Martin V.

6. REPORT DATE	7a. TOTAL NO. OF PAGES	7b. NO. OF REFS
April 1968	38	34

8a. CONTRACT OR GRANT NO. F33615-67-C-1287 b. PROJECT NO. 1471 c. 147102 d.	9a. ORIGINATOR'S REPORT NUMBER(S) WR 67-15 9b. OTHER REPORT NO(S) (Any other numbers that may be assigned this report) AFFDL-TR-67-167

10. AVAILABILITY/LIMITATION NOTICES

This document is subject to special export controls and each transmittal to foreign governments or foreign nationals may be made only with prior approval of the Flight Dynamics Laboratory (FDDA) Wright-Patterson Air Force Base, Ohio 45433

11. SUPPLEMENTARY NOTES	12. SPONSORING MILITARY ACTIVITY
	Air Force Flight Dynamics Laboratory Wright-Patterson AFB, Ohio 45433

13. ABSTRACT

The pressure fluctuations beneath equilibrium boundary layers at subsonic and supersonic speeds are reviewed. Empirical formulae are presented for the intensity, spectra, and cross spectra of the fluctuations. The formulae are intended for direct use in structural response calculations. A simple theoretical model to predict intensities at supersonic speeds is put forward, and the effects of nonequilibrium boundary layers are discussed in general terms. An appendix gives theoretical justification for negative exponential correlation curves at large spacings.

DD FORM 1 JAN 64 1473

Unclassified

Security Classification

Unclassified

Security Classification

14. KEY WORDS	LINK A		LINK B		LINK C	
	ROLE	WT	ROLE	WT	ROLE	WT
Pressure Fluctuations Turbulent Boundary Layer Prediction Techniques Sonic Fatigue						

INSTRUCTIONS

1. ORIGINATING ACTIVITY: Enter the name and address of the contractor, subcontractor, grantee, Department of Defense activity or other organization *(corporate author)* issuing the report.

2a. REPORT SECURITY CLASSIFICATION: Enter the overall security classification of the report. Indicate whether "Restricted Data" is included. Marking is to be in accordance with appropriate security regulations.

2b. GROUP: Automatic downgrading is specified in DoD Directive 5200.10 and Armed Forces Industrial Manual. Enter the group number. Also, when applicable, show that optional markings have been used for Group 3 and Group 4 as authorized.

3. REPORT TITLE: Enter the complete report title in all capital letters. Titles in all cases should be unclassified. If a meaningful title cannot be selected without classification, show title classification in all capitals in parenthesis immediately following the title.

4. DESCRIPTIVE NOTES: If appropriate, enter the type of report, e.g., interim, progress, summary, annual, or final. Give the inclusive dates when a specific reporting period is covered.

5. AUTHOR(S): Enter the name(s) of author(s) as shown on or in the report. Enter last name, first name, middle initial. If military, show rank and branch of service. The name of the principal author is an absolute minimum requirement.

6. REPORT DATE: Enter the date of the report as day, month, year; or month, year. If more than one date appears on the report, use date of publication.

7a. TOTAL NUMBER OF PAGES: The total page count should follow normal pagination procedures, i.e., enter the number of pages containing information.

7b. NUMBER OF REFERENCES: Enter the total number of references cited in the report.

8a. CONTRACT OR GRANT NUMBER: If appropriate, enter the applicable number of the contract or grant under which the report was written.

8b, 8c, & 8d. PROJECT NUMBER: Enter the appropriate military department identification, such as project number, subproject number, system numbers, task number, etc.

9a. ORIGINATOR'S REPORT NUMBER(S): Enter the official report number by which the document will be identified and controlled by the originating activity. This number must be unique to this report.

9b. OTHER REPORT NUMBER(S): If the report has been assigned any other report numbers *(either by the originator or by the sponsor)*, also enter this number(s).

10. AVAILABILITY/LIMITATION NOTICES: Enter any limitations on further dissemination of the report, other than those imposed by security classification, using standard statements such as:

(1) "Qualified requesters may obtain copies of this report from DDC."

(2) "Foreign announcement and dissemination of this report by DDC is not authorized."

(3) "U. S. Government agencies may obtain copies of this report directly from DDC. Other qualified DDC users shall request through

_____."

(4) "U. S. military agencies may obtain copies of this report directly from DDC. Other qualified users shall request through

_____."

(5) "All distribution of this report is controlled. Qualified DDC users shall request through

_____."

If the report has been furnished to the Office of Technical Services, Department of Commerce, for sale to the public, indicate this fact and enter the price, if known.

11. SUPPLEMENTARY NOTES: Use for additional explanatory notes.

12. SPONSORING MILITARY ACTIVITY: Enter the name of the departmental project office or laboratory sponsoring *(paying for)* the research and development. Include address.

13. ABSTRACT: Enter an abstract giving a brief and factual summary of the document indicative of the report, even though it may also appear elsewhere in the body of the technical report. If additional space is required, a continuation sheet shall be attached.

It is highly desirable that the abstract of classified reports be unclassified. Each paragraph of the abstract shall end with an indication of the military security classification of the information in the paragraph, represented as *(TS)*, *(S)*, *(C)*, or *(U)*.

There is no limitation on the length of the abstract. However, the suggested length is from 150 to 225 words.

14. KEY WORDS: Key words are technically meaningful terms or short phrases that characterize a report and may be used as index entries for cataloging the report. Key words must be selected so that no security classification is required. Identifiers, such as equipment model designation, trade name, military project code name, geographic location, may be used as key words but will be followed by an indication of technical context. The assignment of links, rules, and weights is optional.

Unclassified

Security Classification